Catena 157 (2017) 388–396

Contents lists available at ScienceDirect

Catena

journal homepage: www.elsevier.com/locate/catena

Spatial and temporal monitoring of soil moisture using surface electrical resistivity tomography in Mediterranean soils

Abdulmohsen S. Alamry[a,b,*], Mark van der Meijde[b], Marleen Noomen[b], Elisabeth A. Addink[c], Rik van Benthem[c], Steven M. de Jong[c]

[a] Aden University, Department of Engineering Geology, PO Box 405, Ataq, Shabwah, Yemen
[b] University of Twente, Faculty of Geo-Information Science and Earth Observation (ITC), Department of Earth Systems Analysis, PO Box 217, 7500 AE Enschede, The Netherlands
[c] Utrecht University, Department of Physical Geography, PO Box 80115, 3508 TC Utrecht, The Netherlands

ARTICLE INFO

Keywords:
Electrical resistivity tomography
ERT
Soil moisture
Mediterranean

ABSTRACTS

ERT techniques are especially promising in (semi-arid) areas with shallow and rocky soils where other methods fail to produce soil moisture maps and to obtain soil profile information. Electrical Resistivity Tomography (ERT) was performed in the Peyne catchment in southern France at four sites located on four different geological substrates. The main objective was to test the usefulness of such geoelectrical method for the assessment of spatial and temporal variability of soil water content and to demarcate subsurface horizontal zones: topsoil, active zone and bedrock. We used time lapse ERT to separate lithological variability from soil moisture content and to evaluate its potential to demarcate subsurface soil horizons. Three measurement campaigns were carried out and field data were collected using the Sting R1/IP advanced resistivity meter with one-channel receiver. We used an array of 28 electrodes with 1 m spacing, which provided reliable resistivity information to a depth of approximately 5.5 m. ERT were followed by soil sampling carried out with a hand auger, directly below the respective geoelectrical profiles. Empirical linear regression was used to determine the specific relationships between volumetric soil moisture of the field samples and electrical resistivity data obtained in situ. Our conclusions are that ERT is a useful technique for providing information on the spatial–temporal variability of water content in semi-arid areas and for reaching depths otherwise inaccessible. In this study we proposed a method to delineate three important different soil zones: topsoil, active zone, bedrock, based on resistivity data. These three layers are essential information in understanding and modelling the interaction between subsurface and vegetation water uptake, particularly in semi-arid regions.

1. Introduction

The climate in the Mediterranean regions -with long dry periods in summer, mild winters and concentrated rainfall events in spring and autumn- is an important control on vegetation growth, which is further influenced by the often marginal and degraded soil conditions. Regional climate change scenarios predict that the extreme character of the Mediterranean climate will increase: higher temperatures, longer periods of drought and more violent concentrated rainfall events (Gao and Giorgi, 2008). These changing environmental conditions will probably have a deteriorating impact on the Mediterranean ecosystems and landscapes. Annual average precipitation will not change much, but the distribution of precipitation over the year will shift to a stronger seasonal character with dryer summers and more humid winters and furthermore, a shift towards shorter and more intense rainfall events. For vegetation growth, these climate changes will cause decreased water availability during the summer growing season (Nijland, 2011). The dependence of vegetation on soil water storage will therefore increase.

Water availability is an important constraint on vegetation growth in arid and semi-arid regions. During prolonged periods of summer drought, water stored in the soil column is the only available water source for plants and trees. If the soil moisture content drops below a certain level, stomatal closure is induced to reduce water loss, prohibiting photosynthesis (Damesin and Rambal, 1995; Hoff et al., 2002). A drought-induced growth stop is common in Mediterranean regions and this limits ecosystem productivity. Water available in the soil for plants is a function of the precipitation, water retention capacity of the soil (pore space, effective depth or active zone), the root distribution of tree, shrubs and plants in the soil, and the ability of water to flow towards the roots i.e. water conductivity (Lambers et al., 1998). Mediterranean

* Corresponding author at: Aden University, Department of Engineering Geology, PO Box 405, Ataq, Shabwah, Yemen.
E-mail address: alamry1972@yahoo.com (A.S. Alamry).

http://dx.doi.org/10.1016/j.catena.2017.06.001
Received 6 October 2016; Received in revised form 25 May 2017; Accepted 1 June 2017
Available online 06 June 2017
0341-8162/

areas are especially difficult for plants due to the uneven distribution of precipitation in time (relative wet winters and dry summers) and shallow eroded soils (Driessen et al., 2001; Bonfils, 1993).

Information on soil water content and its spatial temporal distribution is crucial for studying primary productivity of these vegetation types and to assess by model simulations the impact of global change on the productivity, the health status and the composition of Mediterranean vegetation. We anticipate that the here proposed Electrical Resistivity Tomography (ERT) approach will yield quantitative information on soil moisture content and allow us to follow soil moisture content over time, and will furthermore provide us with information about the depth of the active zone where water is stored and where the majority of the roots extract plant water.

ERT is documented as a non-invasive geophysical soil survey and monitoring method. It has been used to delineate solute plumes (de Franco et al., 2009; Clement et al., 2010), monitor flow in the unsaturated zone (Barker and Moore, 1998; Binley et al., 2001; Arora and Ahmed, 2011), determine soil water deficit and plant available water (Brunet et al., 2010), study root distribution and root water uptake (Rossi et al., 2011; Srayeddin and Doussan, 2009), define horizon location and stratification (Vanwalleghem et al., 2010; Chaplot et al., 2010), observe soil water dynamics (Nijland et al., 2010; Amato et al., 2009) defining depth to bedrock (Coulouma et al., 2012; Shafique et al., 2011), and used to characterize active-layer depth, soil-moisture content, and permafrost variability (Hubbard et al., 2013).

The main aim of this study was to test the usefulness of the ERT method for the assessment of spatial and temporal variability of soil water content along the transects and to demarcate horizontal zones in the soil profile (top layer, active layer and bedrock) based on differences of resistivity.

2. Materials and methods

2.1. Site description

The study area is located in the Peyne catchment, southern France (Fig. 1) which is characterized by Mediterranean climate. Annual average precipitation is 800–1000 mm and is concentrated in spring and fall. The catchment is situated at the edge of the 'Montagne Noir' and is characterized by a high spatial variation of geological bedrock. Four lithologies were investigated during the ERT experiments: flysch, basalt, marine sandstone, and river terrace sediments (Alabouvette, 1982).

In 2011, we made 12 ERT profiles for 4 sites on four different geological substrates in the beginning and the end of September and the end of October. At each site, we also registered detailed descriptions of soil pits, and obtained gravimetric soil moisture samples. The study area is covered with (semi)natural and agricultural vegetation, mostly vineyards and pasture. The vegetation mainly consists of evergreen shrubs and trees like *Quercus ilex* and *Buxus sempervirens* and is sclerophyll. Three profile sites were chosen in naturally vegetated areas with no recent disturbance and one located in a vineyard-cultivated area.

2.2. ERT

Electrical resistivity tomography (ERT) is a non-invasive geophysical technique for measuring lateral and vertical variation of subsurface electrical resistivity. ERT was selected because, in contrast to most other geophysical methods, like Ground Penetrating Radar (GPR), magnetic susceptibility (MS), gravimetric soil moisture assessment, it provides good information on soil water and can demarcate vertical changes of subsurface soil horizons in the stony soils as found in this region (Nijland et al., 2010; Coulouma et al., 2012). Resistivity measurements are made by inserting an electrical current (I) through two metallic electrodes and measuring the potential difference (ΔV) between two other electrodes (Fig. 2). A single quadruple yields a single value of resistivity, attributed to a single soil volume with dimension and depth defined by the spacing between electrodes and by the configuration used.

Combining measurements of many different electrode combinations along a line allows the calculation of the 2D distribution of electrical resistivity along the transect (Nijland et al., 2010). For 2D ERT surveys, Schlumberger, Wenner and dipole-dipole are the electrode arrays that are the most commonly used. For this study the Schlumberger array was used for its resolving power in both vertical and lateral direction. The measured electrical resistivity of the prospected medium is called apparent resistivity (ρ_a) (Lowrie, 2007):

$$\rho_a = \frac{(AB/2)^2 - (MN/2)^2}{MN} * \frac{\pi \Delta V}{I}$$

where, AB: current electrodes spacing (in m); MN: potential electrodes spacing (in m); ΔV: potential difference (in volts) and I: current (in ampere).

The patterns of resistivity in the soil result from lithology, porosity, structure, temperature, and water content (Lowrie, 2007), all of which differ between regolith and bedrock (Chaplot et al., 2010).

Three geoelectrical measurement campaigns were carried out on four geological substrates. They were performed at the following dates: 5 and 6 September 2011, 21 and 22 September 2011 and 25 and 26 October 2011. In each survey campaign, four 2D electrical resistivity tomography measurements were performed. Data were collected using the Sting R1/IP advanced resistivity meter with one-channel receiver with an array of 28 electrodes with 1 m spacing, which provides reliable resistivity information to a depth of approximately 5.5 m. The electrodes remained in the soil during the whole period of the ERT measurement campaign, also in between periods, to guarantee that measurements were done at exactly the same locations, avoid any electrode polarization changes and to ensure a best quality of measurements (Michot et al., 2003).

Raw ERT data were processed using the EarthImager 2D (Version 2.3.4) software package. EarthImager 2D allows the user to control many different inversion parameters (www.agiusa.com). The inverted resistivity sections were achieved with the EarthImager 2D software. This technique was based on the smoothness-constrained least-squares method and it produced 2-D subsurface model from the apparent resistivity section. In the first iteration, a homogeneous earth model was used as a starting model for which the resistivity partial derivative values could be calculated analytically. For subsequent iterations, a quasi-Newton method was used to estimate the partial derivatives which reduced the computer time. In this method, the Jacobian matrices for a homogeneous earth model were used for the first iteration, and the Jacobian matrices for subsequent iterations were estimated by an updating technique. The model consisted of a rectangular grid. The software determined the resistivity of each mesh which gave a calculated electrical resistivity section according to the field measurements. Then we chose instrument settings which, based on preliminary visual analyses, produced ERT models that best represented physical conditions observed in the soil profiles at our site. After a preliminary inversion of each ERT profile, relative data misfit was checked for all data points in an ERT profile. Individual points with more than 20% misfit were removed. Removal of data points from our profiles was extremely rare, however, which is likely the result of very high quality field data. Misfit histograms typically showed all points in a profile having less than 10% relative data misfit. Inversions were stopped after four iterations or by a Root Mean Square (RMS) error reduction of less than or equal to 1.5%, most inversions reached the inversion criteria on iteration three. Extraction of resistivity profiles from the inversion model is done after all processing and inversion. Due to the nature of these measurements, ERT measures bulk properties (see Fig. 2) and not unique resistivity values at unique locations, the retrieved moisture is an average moisture value for a volume equivalent to the size of the inversion cell.

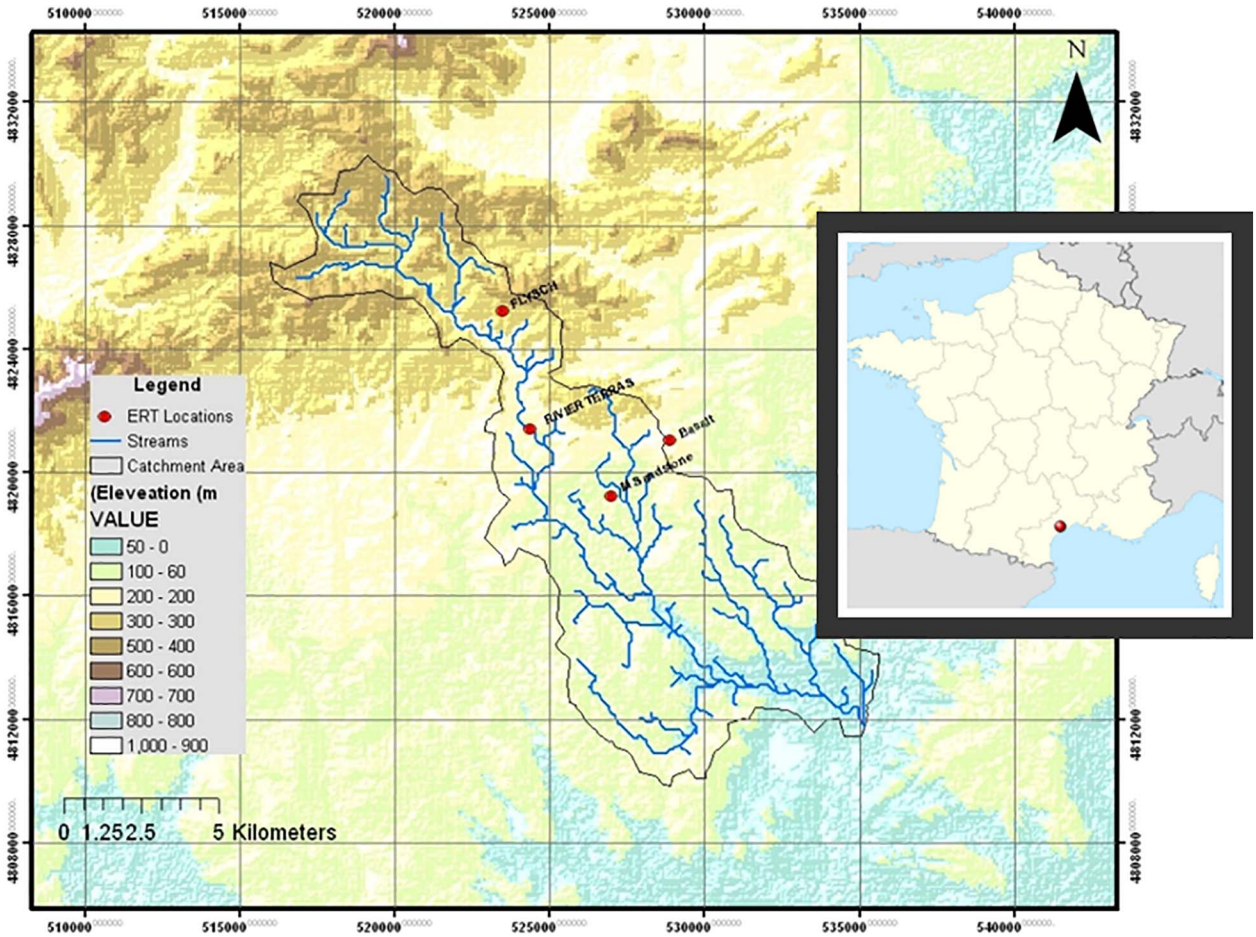

Fig. 1. Location of the study area in southern France.

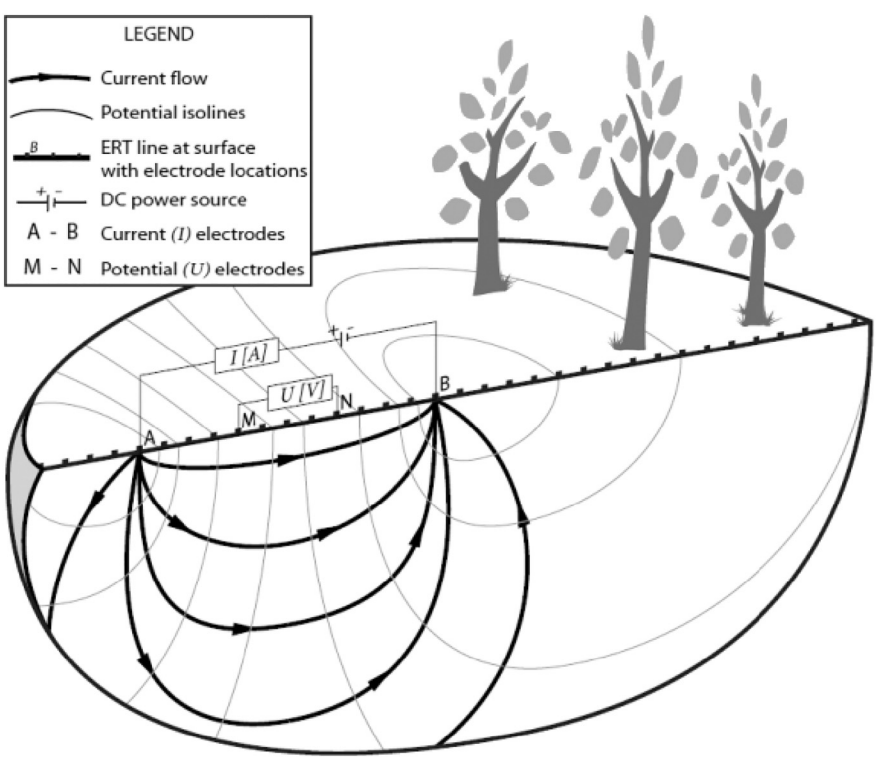

Fig. 2. Schematic diagram of resistivity measurement in a uniform medium. By combining measurements of many electrode combinations using computer tomography, a spatial earth resistivity section is made (After Nijland et al., 2010).

2.3. Soil sampling and moisture analysis

Directly after the ERT surveys, a representative set of soil samples were taken below the ERT profiles on the four geological substrates. A soil pit was dug or drilled as deep as possible using a hand shovel and pickaxe or hand auger. The depths of the pits were constrained by bedrock or very hard soils and reached 50–90 cm. The locations of the pits were selected in a homogeneous and representative part of the profile, based on analysis of the ERT data. Soil pits were used to make a description of the soil profile, and to take soil samples for gravimetric determination of soil moisture content. Soil samples were taken at 10 cm depth intervals, weighed, oven dried, and weighed again. Soil volumetric water content (θ_v) was obtained by multiplying the gravimetric water content (θ_w) with the soil bulk density (Gardner, 1986).

1D resistivity profile data were extracted from the 2D ERT profiles at locations corresponding to soil sample pit data. It was not possible to define an interpolated depth interval for 1D data during extraction, so we used linear interpolation between extracted data elevations to generate 1D resistivity data with the same depth interval, as the pit samples.

2.4. Time-lapse ERT

The primary geophysical method for monitoring the timing and spatial pattern of soil moisture is the time lapse electrical resistivity tomography using a small electrode spacing on the surface. A comparison of resistivity measurements at different moments allows filtering of the ERT signal by the stationary characteristics of the soil and therefore highlights changes in the time-variable soil moisture content. From the variables influencing earth resistivity, moisture is the only one significantly varying on a sub-year timescale and consequently calibrated ERT measurements at different times in the year yield the basis for soil water content mapping.

The short time scale differences of the ERT images (15 days) were used to determine the thickness of topsoil, and long time scale differences of ERT images (49 days) were used to determine the thickness of active zone layer from all the four geological substrates.

3. Results

3.1. ERT – single profile

The ERT profiles from all the different geological substrates show vertical and horizontal variability in soil resistivity (Fig. 3). The upper part of all the soil profiles has wide variations in resistivity values and clearly different resistivity values from the underlying base. The resistivity values from basalt and marine sandstone vary from 42 to 629 and from 6 to 262 Ω-m respectively, (Fig. 3). The resistivity values from flysch and river terrace sediment range from 187 to 920 and 55 to 1193 Ω-m respectively, with lower base resistivity values than the top layer (Fig. 3). The lowest values of electrical resistivity are observed in the ERT profiles from the marine sandstone transect. The measured values for the four substrates match the range of values reported by Nijland et al. (2010).

3.2. ERT and soil moisture estimation

One of the primary objectives of this study was to determine the variation of soil resistivity with volumetric moisture content. Electrical resistivity is a function of a number of soil properties such as texture, water content, clay content and salinity (Samouëlian et al., 2005). Soil resistivity decreases when the water content, clay fraction and salinity increase (Celano et al., 2011; Samouëlian et al., 2005). The electrical resistivity of soils depends on the amount of the water in the pores and on water quality and/or dissolved ions (Samouëlian et al., 2005). In this study we assumed that the electrical conductivity of the pore water remained constant during the period of study.

Empirical non-linear regression was used to determine the specific relationships between gravimetric soil moisture content (θ_v) measured in the laboratory and electrical resistivity data (ρ_a) for the four geological substrates measured in situ. The relationship between ρ_a and θ_v has been successfully used for water content estimation in a number of studies reported in the literature (Binley et al. 2002; Rossi et al., 2011; Michot et al., 2003; Grellier et al., 2007; Celano et al., 2011). The expected relationship of resistivity and soil moisture is inverse, and may be strong enough to show variations in resistivity of the order of $10–10^2$ Ω-m between dry and moist soil (Zhou et al., 2001; Michot et al., 2003). The regression models that best describe the relationship between ρ_a and θ_v are exponential models (Fig. 4). Details on the derived exponential regression models, coefficients of determination and correlation coefficients from the four geological substrates are presented in Table 1.

The data of the basalt transect showed the strongest exponential relationship with a correlation coefficient of determination of $R^2 = 0.98$ followed by flysch $R^2 = 0.91$ and river terrace sediments $R^2 = 0.84$. The relationship observed in the marine sandstone reflects the lowest coefficient of determination ($R^2 = 0.09$), and the data points are scattered. It should be noted that, this site is the vineyard with active land management while the other sites are undisturbed natural vegetation sites. The land management may cause the low correlation for this marine sandstone site covered by vineyards and not the lithological properties itself.

3.3. Spatial and temporal variations of volumetric water content (θ_v)

The regression models between the electrical resistivity (ρ_a) and volumetric water content (θ_v) of Fig. 4 were used for the quantification of θ_v in the topsoil part of the three geological substrates. The topsoil parts of the substrates were selected, because field volumetric moisture data collected in the field were available. Compared to the other substrates the marine sandstone substrate showed a poor relation between (ρ_a) and (θ_v) and was excluded from quantitative temporal comparison. Figs. 5, 6 and 7 show the spatial and temporal variations of volumetric water content along the transects for the upper 50 to 100 cm of the soil profile computed on the basis of the regression functions in Fig. 4 for basalt, flysch and river terrace respectively.

The three figures show important variations in soil moisture contents both in vertical and horizontal directions and between the three substrates. The volumetric water content in the basalt substrate ranges from 0 to 35%, with low values at the right side of the section (Fig. 5). Minor temporal changes have been observed from the basalt transect profile with a tendency to be more dry at the end of September matching intuitive expectations that the soil is drying out at the end of the summer until the autumn rains arrive.

The spatio-temporal patterns of volumetric water content computed for the flysch transect for the 3 different survey dates are shown in Fig. 6. There are only small changes observed between the values from the beginning and the end of September. Towards the end of October, the profile is becoming wetter in the left and right part whereas the central part is drying up. The volumetric water content in the profile varies from 0 to14%.

The spatio-temporal patterns of volumetric water content for the river terrace transect are presented in Fig. 7. The soil moisture shows vertical and horizontal variability with a wet core on the three dates. The volumetric water content ranges from 0 to 11% and minor temporal changes have been also observed.

Although the quantitative values of the soil moisture content should be interpreted with care due to the modest regression between resistivity and in-situ determined moisture content (Fig. 4) some general remarks and trends can be observed in Figs. 4, 5 and 6. Please, note that the color bar has a different scale for the three figures in order to cover the entire range of values. The soil on river terrace has the lowest

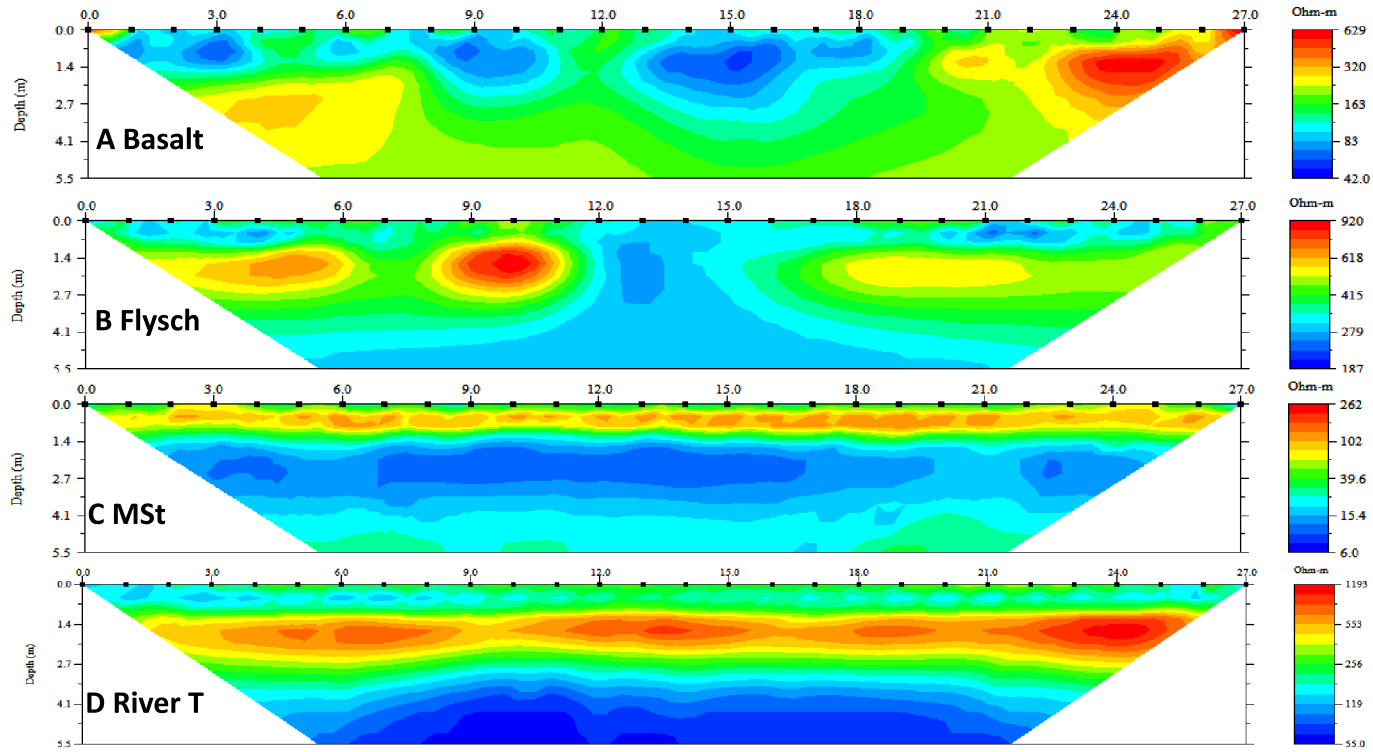

Fig. 3. Example resistivity profiles for all four geological substrates: A: basalt; B: flysch; C: marine sandstone; D: river terrace. Color scales are optimized to the individual profiles. (For interpretation of the references to color in this figure legend, the reader is referred to the web version of this article.)

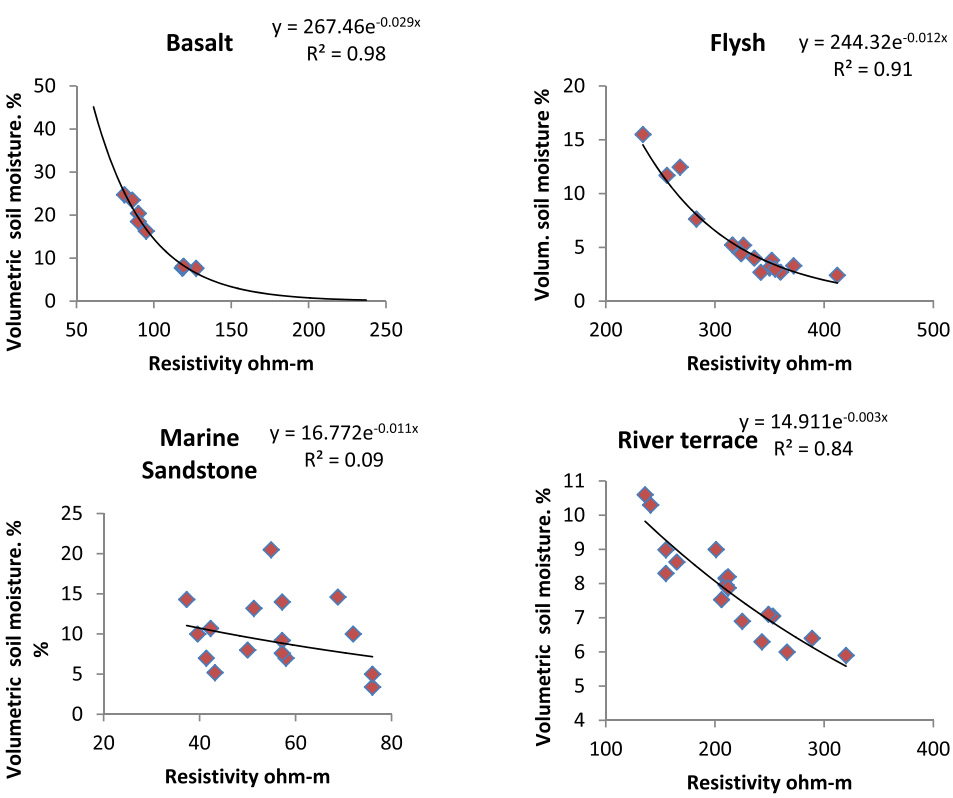

Fig. 4. Relationship between the volumetric water content (θ_v) and the electrical resistivity (ρ_a) for the different geological substrates. Note the difference ranges of the X and Y scales.

moisture content which matches intuitive expectation in coarse textured soils. The soil moisture pattern seems homogenously distributed but given the low moisture values this might also be explained by noisy pattern of these low values. The soil on the flysch substrate of Fig. 5 shows intermediate moisture values. The patterns show a hanging profile indicated draining water deeper into the profile. The spatial patterns along the profile might be caused by the scattered trees along this profile extracting soil water from the profile. The largest range of soil moisture values occurs in the soil on the basalt substrate. The patterns are however biased by two high values locations near meter 15 to 18 and 0 to 3 m along the transect. Given this bias along the profile the patterns are difficult to explain.

Table 1
Results of the derived exponential regression models, number of samples (n), coefficients of determination, correlation coefficients and the maximum depth of the soil pit used for gravimetric soil moisture sampling for each of the four geological substrates.

Substrate	Model	n	R^2	R	Max depth (cm) of soil pit sampling
Basalt	$\theta_v = 267.46 \times e^{-0.029x}$	11	0.98	0.99	50
Flysch	$\theta_v = 244.32 \times e^{-0.012x}$	16	0.91	0.93	70
Marine sandstone	$\theta_v = 16.772 \times e^{-0.011x}$	16	0.09	0.31	60
River terrace sediments	$\theta_v = 14.911 \times e^{-0.003x}$	18	0.84	0.92	90

3.4. Time-lapse ERT

We used time-lapse ERT to separate lithological variability from soil moisture content and to evaluate its potential for demarcating subsurface horizontal zones. As the three ERT temporal profiles were conducted at exactly the same location, it is assumed that the lithology remained unchanged during the period of study and all the observed resistivity changes could be related to soil moisture variations (Nijland et al., 2010).

Fig. 5a shows the ERT difference profile between beginning and end of September for the river terrace substrate as an example for short time-scale differences of ERT images (15 days). The thickness of the topsoil can visually be demarcated very well in the difference image and is shown by the dashed black line. Fig. 8b shows the ERT difference profile between the beginning of September and the end of October 2011 for the river terrace substrate. The thickness of the active zone layer was estimated using the longtime scale differences (49 days) of ERT measurements and indicated by the two black dashed lines in Fig. 8b.

The extracted 1D resistivity log (Fig. 9) at different points from the profiles for three dates were used to confirm thicknesses of the topsoil and the active layer zone and to demarcate depth to bedrock from the four geological substrates. Cross-over points between the 1D profiles from different times are used as boundary indicators for the topsoil, active zone and bedrock (Fig. 9). The time-lapse ERT from flysch substrate is shown as an example. The average thicknesses of the subsurface layers estimated from different location of 1D resistivity logs of ERT profiles are given in Table 2. The common pattern shows a three-layer profile: a top layer with a high lateral variability, a second layer with a maximum change (Active zone) and a base with no change at all. The depth of each zone is different for each of the geological substrates in the study area (Table 2). All the difference profiles show an increase of resistivity in the zone down to 4 m.

The average thickness of topsoil layer predicted from the described ERT method was visually compared with measured thickness in the field derived from the dug soil pits and from auger information and corresponds quite well. The maximum thickness of topsoil layer was observed in the river terrace sediment, maximum thickness of active zone was observed in basalt and flysch substrates, whereas the minimum thickness of the active zone was found in the marine sandstone substrate.

4. Discussion

ERT was used for spatial and temporal monitoring of soil moisture and delimitation of subsurface layer zones, in a semiarid area. Images of the soil electrical resistivity acquired by the ERT technique revealed horizontal and vertical heterogeneities, and temporal variations. Absolute values of soil electrical resistivity largely differed between the four geological substrates. The temporal variations of resistivity reflect variations in water content due to evaporation, drainage and/or variations in water uptake by plants.

The best empirical exponential relationship found in this study is between soil water content and ERT data for the basalt substrate. Results for basalt are probably best due to the low clay content and relatively thin topsoil of this substrate. The decrease of resistivity with higher soil clay contents was earlier observed in studies of clay-rich materials (Robain et al., 2003; Giao et al., 2003; Shah and Singh, 2005). The relative high clay content of marine sandstone for our study area (Alabouvette, 1982; Bonfils, 1993) could be the main reason for the absence of a good relationship between ρa and θv for this formation (Fig. 4). The reason is that clays have the capacity to adsorb large amounts of ions, and hence even small amounts of clay present in the soil may largely lower the electrical resistivity of a soil (Waxman and Smits, 1968). The marine sandstone and to a lesser extend the river terrace are layered formations due to the sedimentation processes in the past. The layered structure has an effect on the ERT response and is visible in Fig. 3c and d. The layered structure remains also visible in the time lapse of ERT in Fig. 7. So, a layered structure of soil substrate will have an impact on ERT response and water content estimates. This study did not have the data available to investigate this effect in a quantitative way but is a topic for further study.

ERT measurements for soil moisture detection are especially useful when applied in a monitoring setting, because by comparing the measurements over time it is possible to separate the effects of moisture and lithology on measured resistivity. For locations with rocky soils like our study site in Mediterranean Southern France it is difficult to get absolute measurements of soil moisture by e.g. gravimetric methods, the benefit of using ERT is that it provides spatial quantitative data from

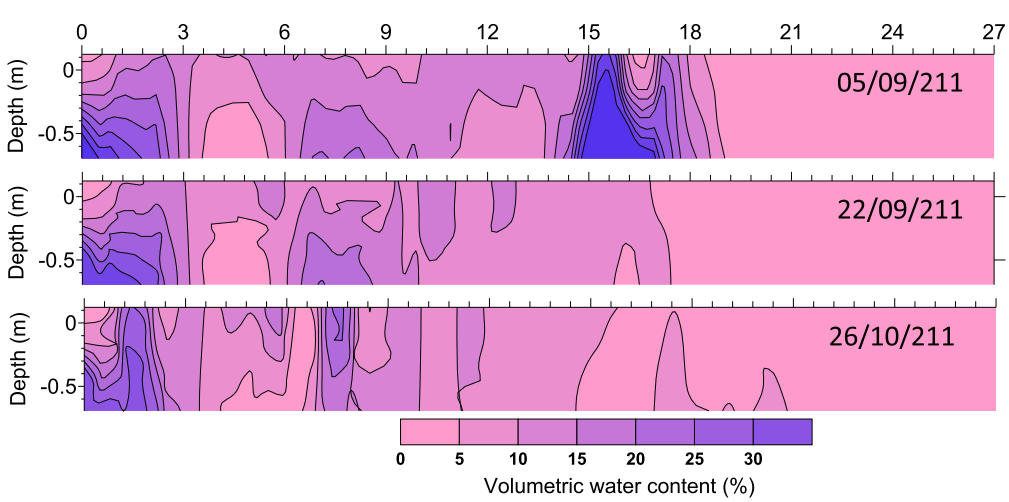

Fig. 5. The spatial and temporal variations of moisture content of topsoil section from basalt substrate.

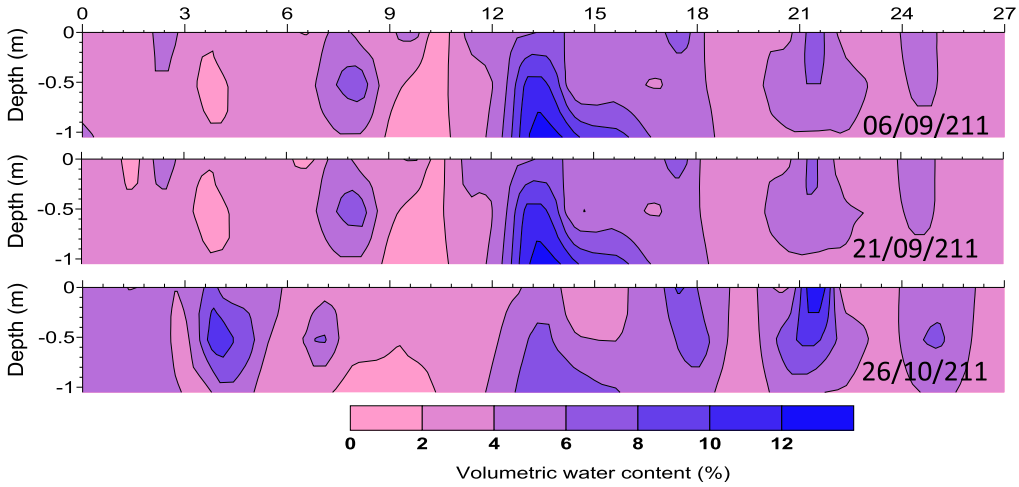

Fig. 6. The spatial and temporal variations of moisture content of topsoil section from flysch substrate.

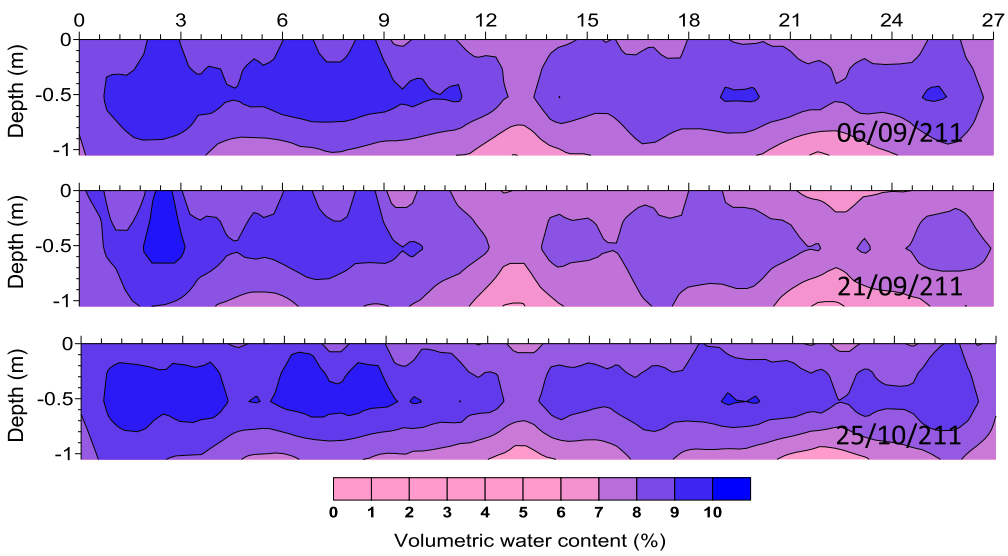

Fig. 7. The spatial and temporal variations of moisture content of topsoil section from river terrace substrate.

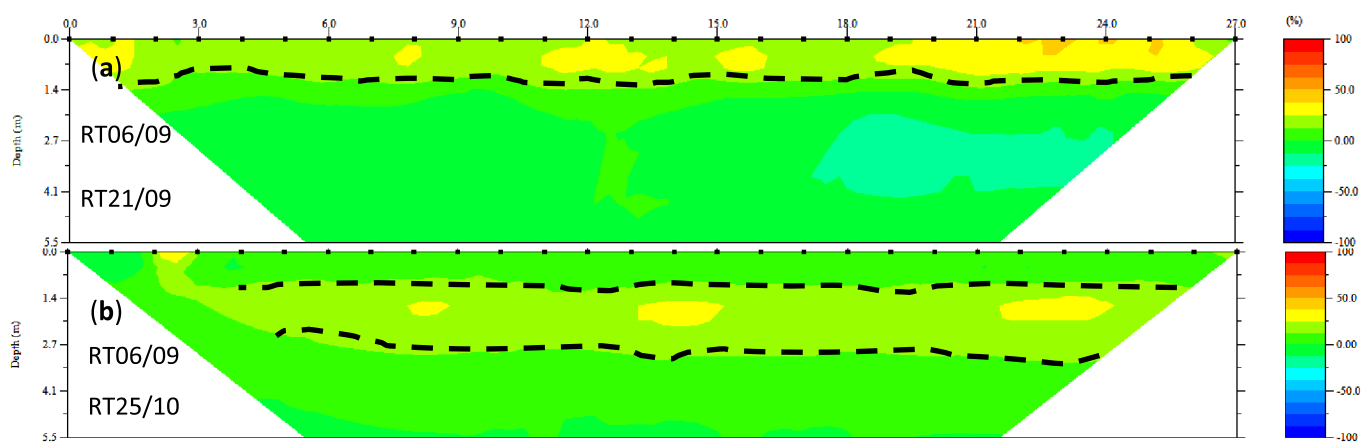

Fig. 8. Time lapse of Electric Resistivity Tomography in situ measurements for the river terrace substrate. a) shows the short time scale differences of 15 days. b) shows the long time scale differences of 49 days. The two difference images allow us to separate the topsoil layer and the active zone soil layer.

otherwise unreachable soil depths.

The detection of subsurface layers using geophysical methods depends greatly on the definition of the layer and the layer properties. ERT is generally used in detection of bedrock in contrasting areas, such as clayey soils developed over limestone (Zhou et al., 2000) or weathered soils over magmatic materials (Beauvais et al., 2007). In such conditions, the differences in electrical resistivity between bedrock and soil are large and layer identification is straightforward. A recent study based on the combination of seismic and electric methods was used successfully for predicting bedrock depth along a Mediterranean soil topo-sequence (Coulouma et al., 2012). In our case, the contrast in resistivity derived from multi-temporal ERT images combined with the data of extracted 1D resistivity logs (profiles), were used to demarcate the subsurface soil zones.

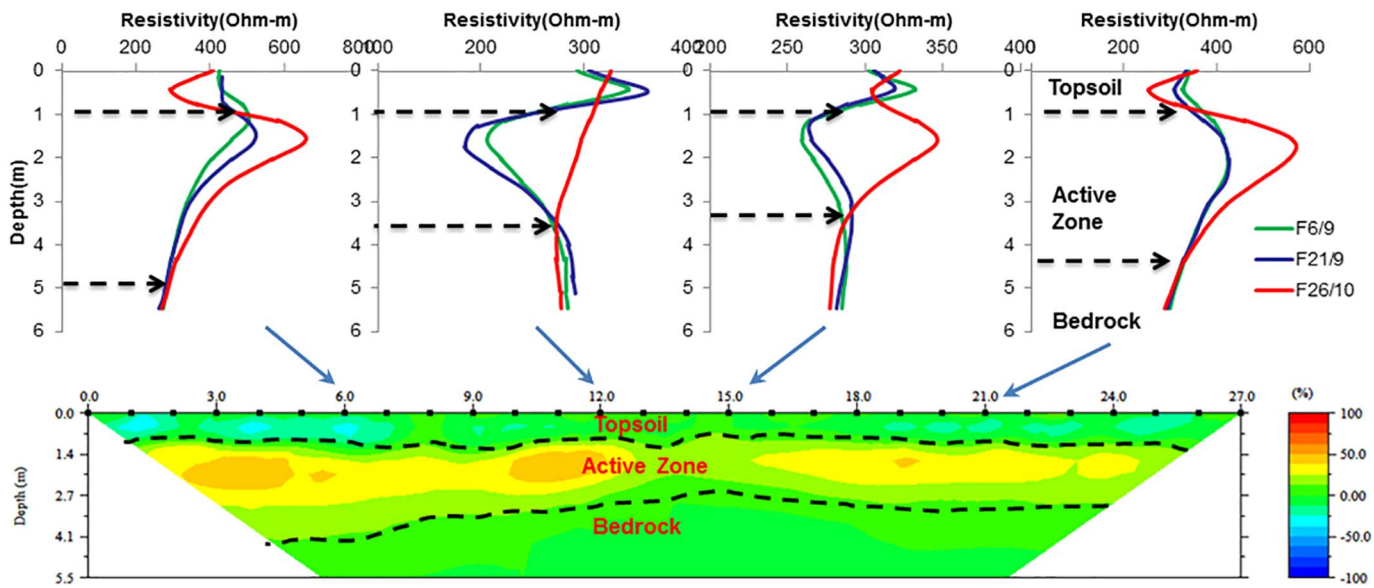

Fig. 9. The extracted 1D resistivity profile at different points along the transect indicated by the blue arrows at 6, 12, 15 and 21 m for the flysch substrate and for the three dates: 6 and 21 September and 26 October. The black arrows in the profile at the four locations indicate the interpreted position of the topsoil, active layer and bedrock. (For interpretation of the references to color in this figure legend, the reader is referred to the web version of this article.)

Table 2
The by ERT estimated average thicknesses of the subsurface layers.

Substrate	Average thickness of topsoil (m)	Average depth to bedrock (m)	Average thickness of active zone (m)
Basalt	0.49	3.74	3.25
Flysch	0.71	3.97	3.26
Marin Sandstone	0.54	2.35	1.81
River terrace sediment	0.89	3.55	2.66

Electrical resistivity values measured for the three dates were plotted against soil depth for every meter of the four substrates. The topsoil is usually less compact than the underlying subsoil, is cracked, loose with dense roots, and has a higher variability and clearly different resistivity values compared to the underlying layers. The ERT data were analyzed to define the topsoil zone hypothetically corresponding to the zone of high variability in resistivity. Topsoil variability in resistivity is probably caused by vegetation and root distribution and the resulting irregular water demand or inhomogeneous moisture pattern (Igel, 2008). The lower limit of the active zone (depth to bedrock) has been demarcated as the boundary below which no significant differences of resistivity between 3 dates conditions were observed (Fig. 9).

The here presented method and results may also be useful to determine the soil depth where plants actively subtract water from the profile. The multi-temporal profile illustrates that plants mainly extract water from the second soil layer earlier referred to as the active zone. Our results match results described by Nijland et al. (2010), they found for flysch and basalts substrates that water extraction by vegetation takes place up to 4 m deep with a maximum extraction around 2 m. ERT is a promising technique to improve our understanding of soil water extraction by plants.

5. Conclusions

In this study we used electrical resistivity tomography (ERT) to monitor spatial and temporal soil moisture in a semi-arid area on four different geological substrates. ERT has proven to be a useful technique for the detection of soil moisture and delineate the different soil moisture zones in non-accessible soils and weathered substrates. We proposed a novel method to delineate vertically and horizontally along the transect, the different soil moisture zones (topsoil, active zone, bedrock) based on resistivity data. The separation of these layers is essential information for understanding vegetation water uptake from these rocky, difficult to penetrate soils and to simulate primary productivity of the vegetation.

The soil water content can be calculated from the ERT data using empirical, lithology-specific relations between the electrical resistivity and volumetric soil water content determined by the gravimetric method. This relationship was significant and allowed to assess spatial–temporal variability of water content in wide and representative soil volumes, which are studied with difficulty by means of traditional and punctual methods of investigation (i.e., gravimetric method, TDR). Our findings show that lithology is an important factor controlling water availability, water storage capacity, and maximum root penetration depth of Mediterranean vegetation.

Acknowledgments

The authors acknowledge the Erasmus Mundus lot 8 program for the scholarship given to the first author.

References

Alabouvette, B., 1982. Carte Geologique de la France a 1/50000: feuille de Lodeve.
Amato, M., Bitella, G., Rossi, R., Gómez, J.A., Lovelli, S., Gomes, J.J.F., 2009. Multi-electrode 3D resistivity imaging of alfalfa root zone. Eur. J. Agron. 31, 213–222.
Arora, T., Ahmed, S., 2011. Characterization of recharge through complex vadose zone of a granitic aquifer by time-lapse electrical resistivity tomography. J. Appl. Geophys. 73, 35–44.
Barker, R., Moore, J., 1998. The application of time lapse electrical tomography in groundwater studies. Lead. Edge 17, 1454–1458.
Beauvais, A., Parisot, J., Savin, C., 2007. Ultramafic rock weathering and slope erosion processes in a South West Pacific tropical environment. Geomorphology 83, 1–13.
Binley, A., Winship, P., Middleton, R., Pokar, M., West, J., 2001. Observations of seasonal dynamics in the vadose zone using borehole radar and resistivity. In: Paper Presented at the Annual Symposium on the Application of Geophysics to Engineering and Environmental Problems (SAGEEP). Environ. and Eng. Geophys. Soc, Denver, Colo.
Binley, A., Cassiani, G., Middleton, R., Winship, P., 2002. Vadose zone flow model parameterisation using cross-borehole radar and resistivity imaging. J. Hydrol. 267, 147–159.
Bonfils, P., 1993. Carte Pedologique de la France 1:100000, feuille de Lodeve.
Brunet, P., Clement, R., Bouvier & C., 2010. Monitoring soil water content and deficit using Electrical Resistivity Tomography (ERT) – a case study in the Cevennes area, France. J. Hydrol. 380, 146–153.
Celano, G., Palese, A.M., Ciucci, A., Martorella, E., Vignozzi, N., Xiloyannis, C., 2011. Evaluation of soil water content in tilled and cover-cropped olive orchards by the

geoelectrical technique. Geoderma 163, 163–170.
Chaplot, V., Lorentz, S., Podwojewski, P., Jewitt, G., 2010. Digital mapping of A-horizon thickness using the correlation between various soil properties and soil apparent electrical resistivity. Geoderma 157, 154–164.
Clement, R., Descloitres, M., Gunther, T., Oxarango, L., Morra, C., Laurent, J.P., Gourc, J.P., 2010. Improvement of electrical resistivity tomography for leachate injection monitoring. Waste Manag. 30, 452–464.
Coulouma, G., Samyn, K., Grandjean, G., Follain, S., Lagacherie, P., 2012. Combining seismic and electric methods for predicting bedrock depth along a Mediterranean soil toposequence. Geoderma 170, 39–47.
Damesin, C., Rambal, S., 1995. Field study of leaf photosynthetic performance by a Mediterranean deciduous oak tree (*Quercus pubescens*) during a severe summer drought. New Phytol. 131, 159–167.
Driessen, P., Deckers, J., Spaargaren, O., Nachtergaele, F., 2001. Lecture notes on the major soils of the world. In: World Soil Resources Reports (FAO).
de Franco, R., Biella, G., Tosi, L., Teatini, P., Lozej, A., Chiozzotto, B., Giada, M., Rizzetto, F., Claude, C., Mayer, A., 2009. Monitoring the saltwater intrusion by time lapse electrical resistivity tomography: the Chioggia test site (Venice Lagoon, Italy). J. Appl. Geophys. 69, 117–130.
Gao, X., Giorgi, F., 2008. Increased aridity in the Mediterranean region under greenhouse gas forcing estimated from high resolution simulations with a regional climate model. Glob. Planet. Chang. 62, 195–209.
Gardner, W.H., 1986. Water content. In: Methods of Soil Analysis, Part 1. Amer. Soc. Agron. Madison, WI, pp. 493–544.
Giao, P.H., Chung, S.G., Kim, D.Y., Tanaka, H., 2003. Electric imaging and laboratory resistivity testing for geotechnical investigation of Pusan clay deposits. J. Appl. Geophys. 52, 157–175.
Grellier, S., Reddy, K., Gangathulasi, R., Peters, C., 2007. Correlation between electrical resistivity and moisture content of municipal solid waste in bioreator landfill. In: Geotechnical Special Publication. 163. pp. 1–14.
Hoff, C., Rambal, S., Joffre, R., 2002. Simulating carbon and water flows and growth in a Mediterranean evergreen *Quercus ilex* coppice using the FOREST-BGC model. For. Ecol. Manag. 164, 121–136.
Hubbard, S.S., Gangodagamage, C., Dafflon, B., Wainwright, H., Peterson, J., Gusmeroli, A., Ulrich, C., Wu, Y., Wilson, C., Rowland, J., Tweedie, C., Wullschleger, S.D., 2013. Quantifying and relating land-surface and subsurface variability in permafrost environments using LiDAR and surface geophysical datasets. Hydrogeol. J. 21, 149–169.
Igel, J., 2008. The small-scale variability of electrical soil properties − influence on GPR measurements. In: 12th International Conference on Ground Penetrating Radar, June 16–19, 2008, Birmingham, UK.
Lambers, H.F., Stuart III, C., Pons, T.L., 1998. Plant Physiological Ecology. Springer, Verlag New York (540 pp.).
Lowrie, W., 2007. Fundamentals of Geophysics. Cambridge University Press, Cambridge, pp. 392.
Michot, D., Benderitter, Y., Doringy, A., Nicoullaud, B., King, D., Tabbagh, A., 2003. Spatial and temporal monitoring of soil water content with an irrigated corn crop cover using surface electrical resistivity tomography. Water Resour. Res. 39.
Nijland, W., 2011. Mediterranean evergreen vegetation dynamics: detection and modelling of forest and shrub-land development in the Peyne catchment. In: Utrecht Studies in Earth Sciences 2, ((PhD thesis). ISBN 978-90-6266-280-7. 126 pp.).
Nijland, W., van der Meijde, M., Addink, E.A., de Jong, S.M., 2010. Detection of soil moisture and vegetation water abstraction in a Mediterranean natural area using electrical resistivity tomography. Catena 81, 209–216.
Robain, H., Camerlynck, C., Bellier, C., Tabbagh, A., 2003. Laboratory measurements of electrical resistivity versus water content on small soil cores. In: Geophysical Research Abstracts. 5.
Rossi, R., Amato, M., Bitella, G., Bochicchio, R., Ferreira Gomes, J.J., Lovelli, S., Martorella, E., Favale, P., 2011. Electrical resistivity tomography as a non-destructive method for mapping root biomass in an orchard. Eur. J. Soil Sci. 62, 206–215.
Samouëlian, A., Cousin, I., Tabbagh, A., Bruand, A., Richard, G., 2005. Electrical resistivity survey in soil science: a review. Soil Tillage Res. 83, 173–193.
Shafique, M., der Meijde, M.V., Rossiter, D.G., 2011. Geophysical and remote sensing-based approach to model regolith thickness in a data-sparse environment. Catena 87, 11–19.
Shah, P.H., Singh, D.N., 2005. Generalized Archie's Law for estimation of soil electrical conductivity. J. ASTM Inter. 2, 1–20.
Srayeddin, I., Doussan, C., 2009. Estimation of the spatial variability of root water uptake of maize and sorghum at the field scale by electrical resistivity tomography. Plant Soil 319, 185–207.
Vanwalleghem, T., Poesen, J., McBratney, A., Deckers, J., 2010. Spatial variability of soil horizon depth in natural loess-derived soils. Geoderma 157, 37–45.
Waxman, M., Smits, L., 1968. Electrical conductivities in oil-bearing shaly sands. SPE J. 8, 107–122.
Zhou, W., Beck, B., Stephenson, J.B., 2000. Reliability of dipole-dipole electrical resistivity tomography for defining depth to bedrock in covered karst terranes. Environ. Geol. 39, 760–766.
Zhou, Q.Y., Shimada, J., Sato, A., 2001. Three-dimensional spatial and temporal monitoring of soil water content using electrical resistivity tomography. Water Resour. Res. 37, 273–285.